# Long-Term Optical Imaging of Intrinsic Signals in Anesthetized and Awake Monkeys

**Anna W. Roe, PhD**
Department of Psychology
Vanderbilt University, Nashville, TN

NOTES

## Overview

This chapter reviews some exciting new efforts to use intrinsic signal optical imaging methods for long-term studies in anesthetized and awake monkeys. The development of such methodologies opens the door for studying behavioral states (such as attention, motivation, memory, emotion, and other higher order cognitive functions) that are unsuitable for study under anesthesia. Long-term imaging also is ideal for studying changes in the brain that accompany development, plasticity, and learning.

This chapter will be restricted to the imaging of intrinsic optical signals in vivo (i.e., without the use of dyes, cf. Grinvald chapter in this book). Although intrinsic imaging lacks the temporal resolution offered by dyes, it is a high spatial resolution imaging method that does not require application of any external agents to the brain. The bulk of procedures described here has been developed in the monkey, but can be applied to the study of surface structures in any in vivo preparation. All procedures described were conducted in accordance with National Institutes of Health guidelines and approved by institutional Animal Care and Use Committees.

## Introduction

The intrinsic signal arises from various sources including changes in blood volume due to local capillary recruitment, activity-dependent changes in the oxygen saturation level of hemoglobin (increase or decrease in deoxyhemoglobin), and light scattering changes that accompany cortical activation (*1*). As these components vary in time course, they can be differentially monitored with different illumination wavelengths. Although functional maps can be obtained at a number of illumination wavelengths, in the monkey visual cortex, the most commonly used is in the range of 600 to 630 nm, wavelengths at which the oxymetry component is relatively large. The intrinsic signal has been associated with so-called "initial dip" in BOLD fMRI studies (*2–7*) and its correlation with neural response, both spiking and subthreshhold neural response, is becoming more firmly established. [For a recent review see (*8*).]

The main computational power in the brain resides in the cerebral cortex, the size and complexity of which serves to differentiate humans from other animals. As each behavior is complex and requires a number of processing stages, the workload of generating sensorimotor behaviors is divided among many different areas; some handle vision, others touch, and yet others higher cognitive functions such as working memory. Within each cortical area, function is parcellated into fundamental compartments or modules. The organization and function of these modules has been an area of active investigation (e.g., 9).

One of the challenges of optical imaging is to understand the modular basis of cognition. How do networks of modules within and across cortical areas achieve vision or memory or emotion? Visualization of such modular activations during behavior is tantamount to watching the brain at work. Over the past decade, researchers have developed methods to visualize activations through implanted "windows on the brain." By applying these methods to the awake, behaving animal, it is hoped that this method can open new vistas in our understanding of the neural basis of cognitive function. Furthermore, the ability of these studies to forge a critical link between a large body of work on animal models and functional imaging in humans will be invaluable.

### Is optical imaging in awake animals feasible?

In 1991, Grinvald and colleagues imaged ocular dominance maps in the awake, untrained monkey (*10*). This pioneering study demonstrated that optical imaging could be performed in the awake animal. Ocular dominance, orientation, and color maps were obtained in the awake, fixating monkey by Vnek *et al.* (*11*). Optical imaging also has been used to demonstrate novel organization in the parietal cortex. Siegel *et al.* (*12*) demonstrated an organization for eye gaze position in Area 7 in macaque monkeys. These and other studies described in this chapter indicate that optical imaging is emerging as a useful tool for examining cortical function in behaving animals.

## The challenge

To maintain a clear, unobstructed view of the cortex, the skull, and dura mater must be prevented from regrowing over the exposed cortex. Furthermore, as part of a "healing response," cortex that is exposed for extended periods of time exhibits a growth of "neo-membrane," a new membrane on the surface of the cortex which seriously degrades the quality of the optical signal. Exposed cortex is also subject to added risk for infection and mechanical injury. Optimally, one needs to develop an implant method that permits routine, repeated imaging sessions in the anesthetized animal or in the awake, behaving animal. Although in smaller animals (e.g., rats, tree shrews, cats) with thin dura, intrinsic optical signals can be imaged through the intact dura or even through the thinned bone (*13–15*), the thickness of the bone and native dura in old world primates makes this option impractical (*10*, personal observations). Different methods using fiber optics have been explored for recording deep structures in the brain (*16*).

To achieve the ability to image the brain long-term, both issues of biology and instrumentation must be dealt with. Several goals need to be achieved:
1) A method of implanting an optically clear artificial dura, such that a cortical area may be imaged

NOTES

over a long (months, years) period of time without infection or regrowth,
2) Development of hardware and software necessary to interface image acquisition, behavioral training, and stimulus presentation systems,
3) Minimization of motion: ways to ensure high mechanical rigidity of camera relative to the brain, minimization of brain pulsations,
4) Training animal to sit sufficiently calmly during image acquisition (for both mechanical and physiological stability),
5) Image alignment and deformation algorithms which allow the summing of images acquired in separate imaging sessions (for improvement of signal-to-noise),
6) Signal enhancing data analysis algorithms and statistical evaluations of signal significance, and
7) Large volume data management routines (5–15Gb collected daily).

## The chamber and artificial dura design

Two models of chamber and artificial dura have been developed to date. Both have successfully enabled long-term imaging of the cortex. The model developed by Grinvald and colleagues (*10*) and also used by Siegel and colleagues (*12*) is derived from the traditional stainless steel chamber design. In this method, an X cut is made in the dura and the four leaves pulled up and glued to the inner wall of the steel chamber. An artificial silicone-based pre-molded hat-shaped dura is then implanted and secured with a rubber silicone ring (*17*).

The second model is a nylon prototype designed for electrophysiological and MRI recordings (*18*) (Figure 1). The top of the chamber is threaded on the inside so that a cap, made of the same material, screws into the chamber securely and provides a good seal (Figure 1E). The bottom of the chamber consists of a number of flexible flanges (Figure 1B) that snap snugly into the craniotomy and, once in, is secure and immovable. This chamber has a low profile on the head, is lightweight and suitable for smaller animals, MRI-compatible, and requires little dental cement and no screws. The artificial dura used in conjunction with this design is a transparent, soft, thermoplastic polyurethane (Tecoflex®) (*19*). This material is completely inert and can be implanted for months to years without reactive growth (*20–22*). In this case, the dura is resected and the base of the dura hat is inserted between the native dura edge and the cortex (Figure 1A). The wall of the hat prevents ingrowth of any native dura into the chamber.

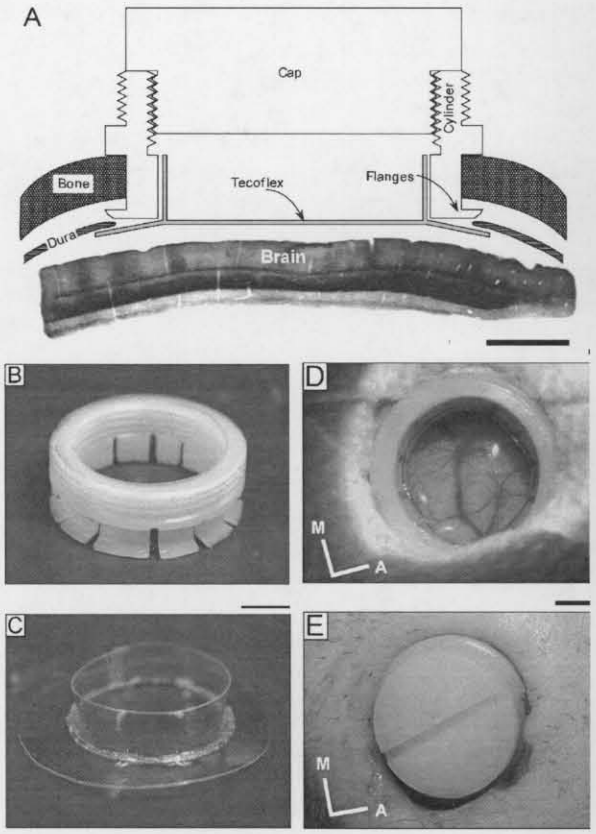


Fig. 1 (A) Profile of chamber and artificial dura over the brain. (B) Chamber. (C) Artificial dura. (D) Chamber open. (E) Chamber closed. [From Chen *et al.*, 2002 (*18*).]

## Long-term maintenance of healthy cortex in a chronic chamber

Prior to chamber implantation, for purposes of interpreting subsequent optical images, determining the topographic representation of the exposed cortex with a brief electrophysiological mapping procedure is extremely useful (Figure 1A). Following implantation of chamber and artificial dura, cortex is maintained in a clear and healthy state and vascular patterns remain stable for years. Repeated imaging experiments can be conducted on the same cortex in the same animal. For subsequent electrophysiological recordings, the artificial dura is removed, recordings conducted, and dura hat easily replaced (Figure 2).

Chamber maintenance is essential for long-term recording without infection or excessive dural growth. Aseptic procedures are used at all times. Before opening the chamber, the outside of the chamber is first cleaned with an antiseptic solution. The chamber cap is then removed and the inside rinsed with sterile saline. Even though in most instances no removal of dural growth is necessary, at times a small amount of new dural growth will emerge from between the artificial dural wall and the chamber wall. This growth has a gelatinous

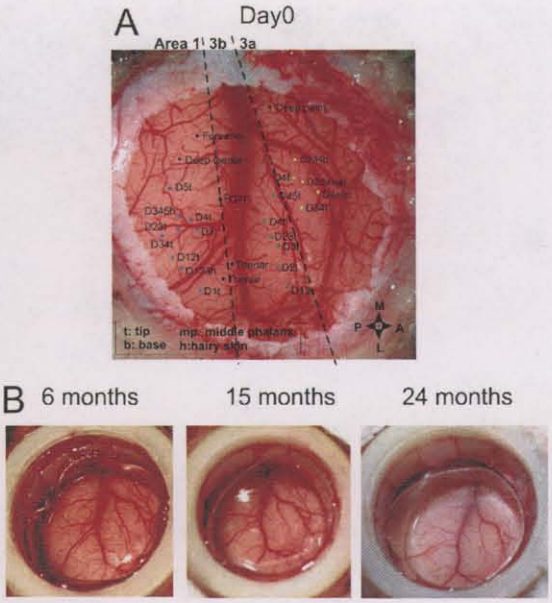


Fig. 2 (A) The dura over SI somatosensory cortex (Area 1, 3b, and 3a) in the squirrel monkey has been resected and a detailed electrophysiological map recorded. (B) Appearance of cortex remains healthy and vascular pattern remains stable for over 2-year period.

consistency and is easily removed with either forceps or cotton swabs. To help prevent infection, a sterile piece of gauze soaked in antibiotic is then placed in the chamber before closing the cap. If these procedures are conducted consistently, problems with dural growth and infection are prevented. In addition, the fluid contents of the chamber should be tested intermittently for bacterial sensitivity, and antibiotics are chosen on the basis of this test. These procedures permit long-term maintenance (years) of healthy imageable cortex (*18, 20–22*).

## Repeated imaging in anesthetized monkeys

### Anesthetic choice.

Intrinsic signal optical imaging is compatible with a wide range of anesthetics, and the anesthetic choice may vary with species, individual, cortical area, and stimulus paradigm. The key to successful optical imaging is maintenance of a stable plane of anesthesia (as measured by heart rate, expired $CO_2$, EEG, blood oxygenation, and blood pressure). This provides conditions optimal for maximizing signal-to-noise ratio. The ideal depth of anesthesia is a Level 2 (light to moderate anesthesia characteristic of sleep). This level is characterized by low frequency, high amplitude (up 150 μV) bursts with periods of suppression less than 1 sec. In humans in this state, the patient has lost consciousness, has reduced reflex activity, has no reaction to painful stimuli, and can undergo surgical procedures. If the subject is too light, the anesthetic plane fluctuates, leading to increased baseline noise. If the subject is too deep, cortical activity is compromised. In our experience, slightly deeper anesthesic planes are preferable over fluctuating anesthetic planes. For imaging in anesthetized monkeys, our anesthetic of choice is sodium pentothal, supplemented lightly with a gas anesthetic (e.g., 0.1 to 1.0 percent isoflurane), which enables rapid micro-adjustments of anesthesia. Imaging can be conducted solely on gas anesthetics, which offer rapid reversibility and fast recovery times for the animal. However, this is accompanied by greater baseline fluctuation than with pentothal. Sufentanil also has been used reversibly for studying higher cortical areas (such as V4) that are typically suppressed under anesthesia (*23*). Other anesthetics such as propofol (*24*), halothane (*25*), and urethane (*14*) also have been used successfully in intrinsic signal optical imaging experiments.

### Stability of maps.

As a measure of the health of the cortex, it is important to establish the stability of the cortical responses to the same stimuli over time (Figure 3).

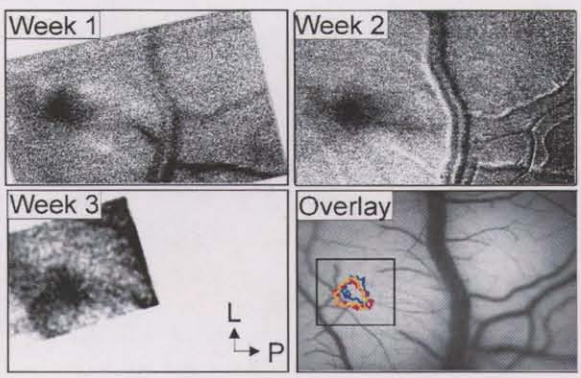


Fig. 3 Cortical responses to tactile indentation on Digit 3 (D3) are imaged repeatedly on three different days. Response region is overlain on blood vessel map (colored lines), which reveals stable topography over time. Signal amplitudes were stable over time (0.77+0.1, 0.83+0.07, and 0.59+0.14 percent).

Stable maps have been reported in both visual and somatosensory cortices (*11, 17, 18, 20*). The amplitudes (0.1 to 1.0 percent) and time courses of optical signal over time remain stable. No significant decline in signal amplitude occurs over a 2-year imaging period.

## Imaging in awake monkeys

### General strategy.

Adult macaque (Macaca fascicularis, Rhesus) and squirrel (Saimiri sciureus) monkeys have been used for awake optical imaging experiments. Monkeys are chronically implanted with optical chambers and head post, and trained to sit calmly in a chair. Visual tasks include visual fixation and tasks requiring eye movement responses such as orientation discrimina-

NOTES

NOTES

tion and delayed match to sample tasks. Tactile tasks in squirrel monkeys have required the monkey to hold the hand still. To permit comparison of anesthetized and awake signals, the same monkeys were imaged in both states. Detailed surgical and optical imaging procedures can be found in (*26, 27*).

### Monkey selection.

In our experience, not all monkeys image equally well. It is widely believed that younger animals have stronger blood-flow related signals; however, there are no systematic studies to test this hypothesis. We thus screen each monkey for imageability before embarking on any training and chamber implantation procedures. For macaque monkeys, we also screen for the availability of V2 exposure (much of V2 is buried in the lunate sulcus and the amount of V2 on the surface of the operculum varies across individuals). Thus, for each monkey, an initial optical imaging procedure is conducted under anesthesia. In macaque monkeys, we examine the number of trials with which ocular dominance, orientation, and color maps are obtained in V1 and V2. In squirrel monkeys, digit tip activation is a reliable marker for imageability. Typically, most monkeys will produce good maps within 20 trials. In stable preparations, it is not uncommon to see ocular dominance in a single trial.

### Monkey training.

Monkeys are implanted with a head post, and then trained to sit calmly in the chair (Figure 4). The animal is rewarded with a drop of juice to reinforce sitting still in the primate chair during training and recording. After training, monkeys are implanted with a chamber and native dura is replaced with transparent artificial dura. For some monkeys, initial sessions may be accompanied by sedation until the animal becomes accustomed to the length of time required for chamber preparation and camera positioning (usually 30 to 60 min). Imaging sessions usually run about 3 h.

### Brain stabilization during imaging.

To minimize pulsations during imaging, we typically use either agar (4 percent) or agar with a transparent silicone wafer. The total time required for chamber preparation can be kept reasonably short (i.e., about 10 to 15 min). Following imaging, the agar is removed, the chamber rinsed with sterile saline, antibiotic applied, and the cap replaced.

### Stimulus presentation.

Visual stimuli include visual gratings of various orientations and spots at different locations in space. Ocular dominance maps are collected using an electromechanical shutter placed in front of the eye. Tactile stimuli are either cutaneous, electrical, or vibrotactile stimulation on the fingertips. Stimuli within each set [including blank (no stim)] conditions are randomly interleaved during image acquisition.

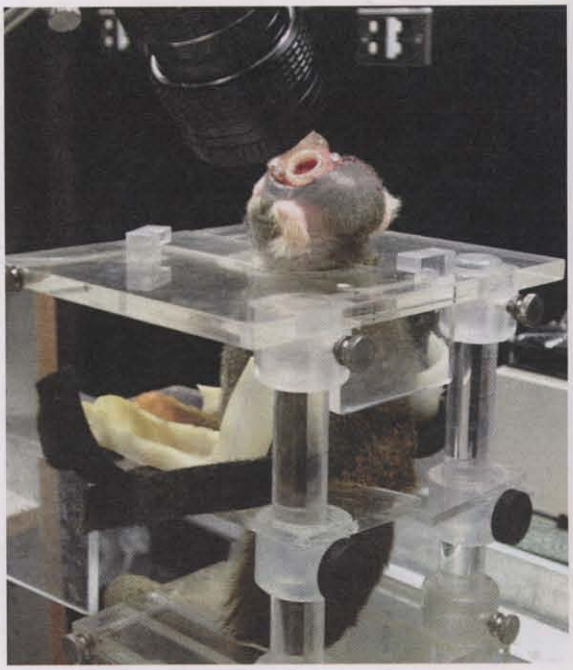

Fig. 4 Optical imaging setup of squirrel monkey with implanted chamber.

### Synchronization with heartbeat and respiration.

Synchronization with heartbeat and respiration is not necessary; these signal artifacts can be minimized by subtraction of pre-stim or blank conditions (*11, 17, 20, 28*).

### Image acquisition.

In our experiments, images were collected using the Imager 2001 and 3001 systems (Optical Imaging Inc., Germantown, NY) and a 630 nm illumination. We are currently developing the NeuroCCD-SM256 system (RedShirtImaging, LLC) for use in the awake, behaving monkey; the camera has an extremely low read noise, high quantum efficiency, a large well depth of 1,000,000, a large spatial 256 x 256 array CCD, and fast readout. In a typical session, depending on the monkey, 50 to 500 trials are collected per stimulus condition. Intrinsic signal maps were collected at 5 to 15 image frames per sec for 3 to 5 sec starting at 200 msec prior to stimulus onset. Inter-stimulus intervals were 6 to 12 sec.

### Comparison of the anesthetized and awake imaging conditions.

Identical stimuli are presented in the anesthetized and awake states. However, significant differences remain. In the anesthetized animal, conditions are optimized such that physiological variability is minimized by careful regulation of anesthesia, cortical pulsations are minimized with agar or

NOTES

silicone oil in an optical chamber, and stimuli are presented in a well-controlled, repeatable fashion. In the awake animal, there is much greater variability of the animal's respiration and heart rate and much greater motion artifact due to both body movements and to greater cortical pulsations, resulting in significant trial to trial variability of the optical signal. Thus, depending on the behavior of the individual monkey, some portion of the trials is discarded due to excessive movement artifact. Response to repeated presentation of stimuli should, with averaging, produce consistent signal more reliably than occasional and erratic signals due to movement or changes in the animal's physiology. Appropriate analyses are conducted to ensure that signal is not due to systematic contribution by sources not related to the stimuli presented (e.g., motion artifact due to licking).

## Image Analysis

Typically, for each stimulus condition, image frames are summed to maximize signal-to-noise ratio. Before summation, images are examined either manually (*10, 11*) or in an automated fashion (*12*) to remove trials that contain excessive noise. Blank condition trials are examined for possible non-stimulus related changes in reflectance. In addition, poor behavioral performance (e.g., excessive body movement, sleeping) also leads to trial exclusion. Control analyses include comparison of sums of different blocks of trials; presence of sporadic high amplitude noise would produce different half-trial maps; whereas, consistent non-artifactual signal would produce similar maps. Consistency of single condition (either blank subtracted or first frame subtracted) analyses and two condition subtraction analyses further establish believability of the signal. Blank subtractions not only measure change from baseline, but also reduce blood vessel artifact and minimize effects of uneven illumination. When used together, we are able to confirm that the imaged signals are consistent and repeatable, and not due to noise signals occurring in one or a few of the trials.

### Determining signal significance.

Methods for determining signal significance include thresholding (*26, 27*), t-maps (*29*), response correlation (*30*), bootstrapping (*12*), and principle components analysis (*31*) methods. In threshholding procedures, images are typically low-pass filtered, pixel distributions established, and the pixels with strongest activations above a certain value (e.g., 15 percent) identified. This method is appropriate for clear, focal activations where different threshold levels produce similar regions of activation (e.g., *32*). High-pass filtering is typically used in cases where gradual gradation of pixel values is observed over the image (i.e., due to illuminant unevenness or to cortical curvature). Masks are commonly used to exclude pixels that have aberrantly large reflectance change (e.g., excluding pixels > 0.5 SD from mean of distribution); this is useful for removing the most offensive large blood vessel noise. It is not acceptable to interpolate pixel values across regions of excluded vasculature (cf. *15, 33*). Correlation of pixel time courses also has been used to determine significance in response (*30*). In a study on the mapping of gaze direction in the parietal lobe, Siegel *et al.* (*12*) devised a method of normalizing every pixel to an initial pre-stimulus baseline and, following outlier rejection, calculating significance from the mean by Monte Carlo analysis. A useful method developed by Wang *et al.* (*29*) generates t-maps, which evaluates, pixel-by-pixel, similarity between trials of pre-stimulus and post-stimulus response using a standard t-test.

## Motion correction

### Linear.

At times, monkey movements may introduce translational noise to the images. It is, therefore, useful to have a motion correction algorithm to "shift back" the frames to the original location and thus permit correct frame alignment before image summation (Figure 5A–C).

This can be done only with original DC frames (not with difference signals typically collected by 8-bit camera, Imager 2001). As can been seen in Figure 5D, frame-to-frame shifts in the anesthetized animal (blue line) are small and periodic, while those in the awake animal (red line) are larger and more erratic. These procedures improve image alignment and appropriate summing of corresponding pixels, and, therefore, increase signal-to-noise in images.

### Non-linear.

From day to day and over long periods, the position and curvature of the cortex may change. Deformation algorithms may also be used for non-linear changes in the cortical map (Figure 6). These procedures increase the number of trials that can be summed beyond those collected within a single session and therefore help to increase signal-to-noise.

## How similar are activation patterns?

In visual cortex, repeated imaging of ocular dominance and orientation in awake monkeys produces fairly stable maps similar to those obtained in the anesthetized state (*11, 17, 28*). In somatosensory cortex, there is significant variability in receptive field size and topography depending on level of alertness/anesthesia, on attentional state, and on activation of local neurotransmitter (especially GABAergic) systems (*34–36*). Indeed, rapid shifts in receptive field organization have been observed (e.g., *37*) and further suggest the dynamic nature of somatosensory

NOTES

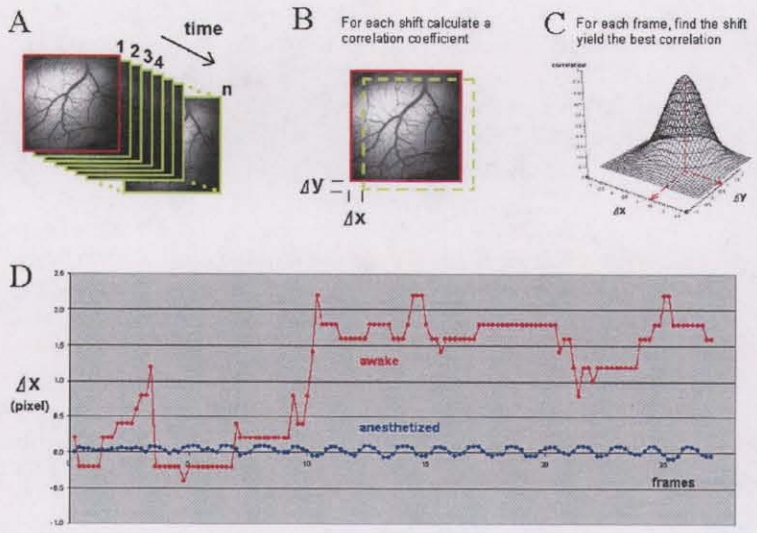


Fig. 5 Motion correction algorithm. (A) Time sequence of image frames. (B) Select one frame as "base" frame (usually the very first frame of the run). Shift each frame in x and y coordinates in 0.2 to 0.5 pixel steps. For each shift, calculate the correlation coefficient between the base frame and current frame. (C) Repeat for every pixel in a small area (e.g., 10 x 10 comparison will give 100 correlation coefficients). Find the best coefficient and use corresponding shift offset (dx, dy). (D) Magnitude of correction in an anesthetized monkey (blue) and an awake, fixating monkey (red) (140 frames over 28 sec).

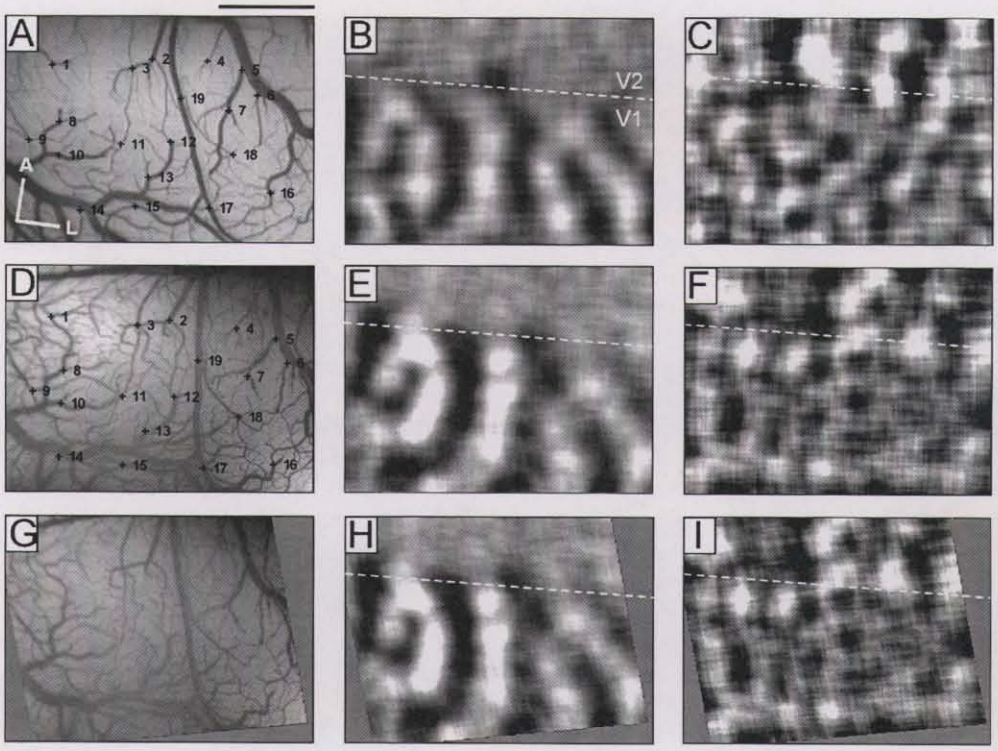


Fig. 6 Ocular dominance (B, E) and orientation (C, F) maps from V1 and V2 in macaque monkey on two different days (A–C versus D–F). Black crosses in A and D indicate the alignment points used to generate transformation function between images. (F-I) Application of transformation to images in A–C produce images similar to D–F. [From Chen *et al.*, 2002 (*18*).]

cortex. Given these differences, we asked how similar topographic and areal activation patterns would be in awake and anesthetized squirrel monkeys.

We find evidence that in somatosensory cortex, activation patterns can differ significantly between anesthetized and awake preparations. In the anesthetized state, we generally observe stronger activations in Area 3b than in Area 1 (Figure 7A). The opposite is observed in the awake state, where Area 1 activations are more prominent (Figure 7B). In fact, in some cases, only Area 1 activation is observed and no apparent Area 3b activation is seen at all.

Topographically, the map in the awake state appears less precise and also different from the map in the anesthetized state. The activations to D3 and D4 stimulation are highly overlapped (Figure 7C).

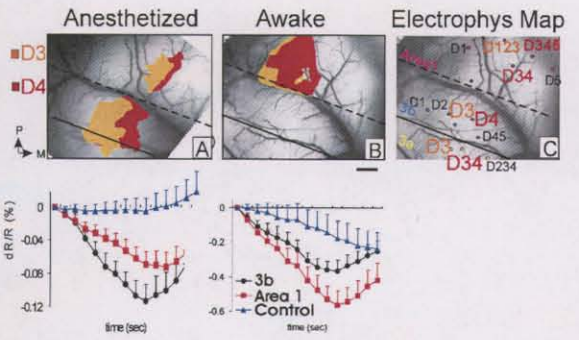


Fig. 7 Cortical response to vibrotactile stimulation of D3 and D4 in the squirrel monkey. (A) Anesthetized activation prominent in Area 3b (see time course below). (B) Awake activation prominent in Area 1 (see time course below). (C) Electrophysiological mapping of Areas 3a, 3b, and 1.

Finally, we observe, within Area 1, a lateral displacement of activation in the awake state from that in the anesthetized state (compare A and B). This result is obtained with both electrical and vibrotactile stimulation (*20*). These results suggest significant awake versus anesthetized differences in somatosensory activations, perhaps due to differences in neural response or vascular response.

## How big is the signal?

### Magnitude, time course, and signal/noise in anesthetized versus awake monkeys.

As shown in Figure 8, the time course of optical signal in both anesthetized and awake squirrel monkey SI cortex peaks at around 2.0 to 2.2 sec post-stimulus onset, and is sustained longer than in the anesthetized animal.

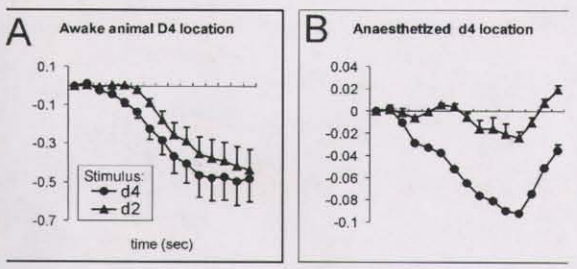


Fig. 8 Time course of optical signal in Area 3b of the squirrel monkey in response to vibrotactile stimulation of digits D2 (circle) and D4 (triangle). Awake (A) and anesthetized (B) signals were obtained from identical location in same monkey to identical stimulus. All signals measured at D4 location.

Consistent with signals obtained in awake visual cortex (*17*), the peak reflectance change in the awake animal is several times larger than in the anesthetized animal. In an average of 12 awake monkey experiments, signal amplitude was 0.92+0.38 percent at the digit center, and 0.38+0.22 percent on a control location away from activation center. In an average of 13 anesthetized monkey experiments, the corresponding numbers are 0.32+0.068 percent on digit center and 0.014+0.017 percent on control location. If one takes the ratio of signal size to error size, this factor is 2.4 (=0.92/0.38) in the awake state and 4.7 (=0.32/0.068) in the anesthetized state. As a measure of discriminability from unstimulated cortex (center/control), the factor is 2.4 (=0.92/0.38) in the awake state and 22.8 (=0.32/0.014) in the anesthetized state. Thus, while signal size is larger in awake animals, noise is also larger by at least a factor of two and discriminability decreases by an order of magnitude. The basis of these differences remains to be investigated.

## Future directions

Optical imaging has been used to elucidate the functional organization of sensory cortical areas in primates. A future goal is to use this methodology to explore functional organization of cognitive functions such as memory. In a preliminary study, we examined the organization for spatial memory in the prefrontal cortex of awake, behaving rhesus macaques using intrinsic signal imaging (*21*). Monkeys performed an oculomotor-delayed response task (Figure 9).

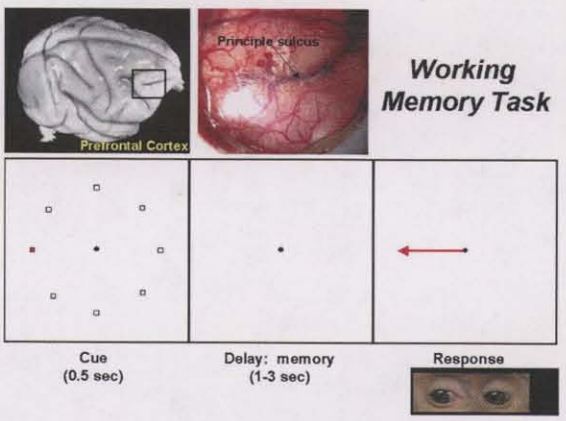


Fig. 9 Oculomotor delayed response task. While fixating on a central spot, the monkey was required to remember the location of a flashed spot (red dot) during the delay period. During the response period, saccade to correct location is rewarded with juice. Images were collected during cue, delay, and response periods.

Up to eight directions and two saccade sizes were used with a 2-sec delay period. We found that cue-period reflectance change varied as a function of distance from the principle sulcus. During the delay period, we observed a response that varied with saccade direction, suggesting a broadly organized topographic map of "memory fields" on the banks of the principal sulcus (*38*). These responses were not observed in the anesthetized prefrontal cortex. Our

NOTES

NOTES

results suggest possible functional organization for memory-related signals in prefrontal cortex and demonstrate a role for optical imaging in examining prefrontal function (39).

## Acknowledgments

Many thanks to Haidong Lu and Limin Chen for assistance with this document. Supported by NEI, NINDS, and Packard Foundation.

## References

1. T Bonhoeffer, A Grinvald, Optical imaging based on intrinsic signals: The methodology. In: *Brain Mapping: The Methods*, Academic Press, AW Toga, JC Mazziota, 55 (1996).
2. I Vanzetta, A Grinvald, *Science* **8286**, 1555–1558 (1999).
3. DS Kim, TQ Duong, SG Kim, *Nat. Neurosci.* **3(2)**, 164–169 (2000).
4. AF Cannestra *et al.*, *Cereb. Cortex* **11(8)**, 773–782 (2001).
5. A Devor *et al.*, *Neuron* **39(2)**, 353–359 (2003).
6. JK Thompson, MR Peterson, RD Freeman, *Science* **299**, 1070–1072 (2003).
7. S Sheth *et al.*, *Neuroimage* **19(3)**, 884–894 (2003).
8. A Zepeda, C Ariasa, F Sengpiel, *J. Neurosci. Methods* **136**, 1–21 (2004).
9. AW Roe, Modular complexity of area V2 in the macaque monkey. In: *The Primate Visual System*, CRC Press, Eds. C Collins, J Kaas, 109–138, (2003).
10. A Grinvald, RD Frostig, RM Siegel, E Bartfeld, *Proc. Natl. Acad. Sci. USA* **88**, 11559–11563 (1991).
11. N Vnek *et al.*, *Proc. Natl. Acad. Sci. USA* **96**, 4057–4060 (1999).
12. RM Siegel *et al.*, *J. Neurophysiol.* **90(2)**, 1279–1294 (2003).
13. RD Frostig, EE Lieke, DY Ts'o, *Proc. Natl. Acad. Sci. USA* **87**, 6082–6086 (1990).
14. AF Cannestra, N Pouratian, MH Shomer, AW Toga, *J. Neurophysiol.* **80(3)**, 1522–1532 (1998).
15. WH Bosking, R Kretz, ML Pucak, D Fitzpatrick, *J. Neurosci.* **20**, 2346–2359 (2000).
16. DM Rector, RF Rogers, JS George, *J. Neurosci. Methods* **91**, 135–145 (1999).
17. E Shtoyerman *et al.*, *J. Neurosci.* **20**, 8111–8121 (2000).
18. LM Chen *et al.*, *J. Neuroscience Methods* **113**, 141–149 (2002).
19. DE Sakas, K Charnvises, LF Borges, NT Zervas, *J. Neurosurg.* **73**, 936–941 (1990).
20. AW Roe *et al.*, *Program* Abstract Viewer/Itinerary Planner, CD-ROM, Washington, DC: Society for Neuroscience, **28** 651.32002 (2002).
21. AW Roe, D Walled, E Sybirska, PS Goldman-Rakic, *Soc. Neurosci. Abstract*, San Diego, CA. (2004).
22. B Heider *et al.*, *Soc. Neurosci. Abstract* **619**, 33 (2001).
23. GM Ghose, DY Ts'o, *J. Neurophysiol.* **77(4)**, 2191–2196 (1997).
24. X Xu *et al.*, *J. Neurosci.* **24(28)**, 6237–6247 (2004).
25. S Schuett, T Bonhoeffer, M Hubener, *Neuron* **32(2)**, 325–337 (2001).
26. BM Ramsden, CP Hung, AW Roe, *Cerebral Cortex* **11** 648–665 (2001).
27. LM Chen *et al.*, *J. Neurophysiol.* **86**, 3011–3029 (2001).
28. H Slovin, A Arieli, R Hildesheim, A Grinvald, *J. Neurophysiol.* **88(6)**, 3421–3438 (2002).
29. G Wang, M Tanifuji, K Tanaka, *Neurosci. Res.* **32**, 33–46 (1998).
30. M Tommerdahl *et al.*, *J. Neurophysiol.* **80**, 3272–3283(1998).
31. L Sirovich, E Kaplan, Analysis methods for optical imaging. In: *Optical Imaging*, CRC Reviews, Ed. R Frostig (2002).
32. TH Schwartz *et al.*, *Neuroreport* **15**, 1527–1532 (2004).
33. DC Lyon *et al.*, *Proc. Natl. Acad. Sci. USA* **99**, 15735–15742 (2002).
34. RW Dykes *et al.*, *Neurosci.* **6**, 1687–1692 (1981).
35. Y Iwamura, M Tanaka, M Sakamoto, O Hikosaka, *Exp. Brain. Res.* **51**, 327–337 (1983).
36. KD Alloway, H Burton, *Exp. Brain. Res.* **85(3)**, 598–610 (1991).
37. CE Schroeder, S Seto, JC Arezzo, PE Garraghty, *J. Neurophysiol.* **74(2)**, 722–732 (1995).
38. S Funahashi, CJ Bruce, PS Goldman-Rakic, *J. Neurophysiol.***61(2)**, 331–349 (1989).
39. E Seidemann, A Arieli, A Grinvald, H Slovin, *Science* **295(5556)**, 862–865 (2002).